ARTICLE IN PRESS

ELSEVIER

Journal of Biomechanics ▮ (▮▮▮▮) ▮▮▮–▮▮▮

JOURNAL OF BIOMECHANICS

www.elsevier.com/locate/jbiomech
www.JBiomech.com

Technical note

A computer algorithm for representing spatial–temporal structure of human motion and a motion generalization method

Woojin Park[a,*], Don B. Chaffin[b], Bernard J. Martin[b], Julian J. Faraway[c]

[a]*Department of Mechanical, Industrial, and Nuclear Engineering, University of Cincinnati, University and Campus Drive-626 Rhodes Hall, Cincinnati, OH 45221-0072, USA*

[b]*Department of Industrial and Operations Engineering, The University of Michigan, 1205 Beal Avenue, Ann Arbor, MI 48109, USA*

[c]*Department of Statistics, The University of Michigan, 459 West Hall, 550 East University, Ann Arbor, MI 48109-1092, USA*

Accepted 23 September 2004

Abstract

Inspired by the generalized motor program (GMP) theory, this study presents a symbolic motion structure representation (SMSR) algorithm that identifies a basic spatial–temporal structure of a human motion. The algorithm resolves each joint angle–time trajectory of a multi-joint motion into a sequence of elemental motion segments and labels each motion segment with a symbol representing its shape ('U': monotonically increasing; 'D': monotonically decreasing; 'S': stationary). By concatenating symbols according to their order in time, the spatial–temporal *structure* of a joint angle–time trajectory is represented as a symbolic string. The structure of a multi-joint motion is then represented as a set of symbolic strings. A sample motion, whose structure is identified by the SMSR algorithm, can be generalized to produce an infinite number of similar motion variants. To generate a variant of a sample motion, segment boundary points of the sample motion are first relocated to new locations in the angle–time space, and then individual motion segments of the original joint angle trajectories are shifted and proportionally rescaled to fit the new segment boundary points. This motion generalization method provides a basis for developing GMP-based motion simulation models, and exploring ideas and hypotheses related to the GMP theory through simulation. As an application of the motion generalization method, a motion modification (MoM) algorithm is presented, which adapts existing reach motions for new target locations. Some examples generated by the MoM algorithm are illustrated.

Keywords: Generalized motor program; Motion structure; Motion generalization; Symbolic representation; Motion simulation; Schema

1. Introduction

The human motor system is able to generalize previously acquired motor skills to plan novel motions. The notion of generalized motor programs (GMPs) has been theorized to account for this capability (Schmidt and Lee, 1999; Schmidt, 1975). A GMP is portrayed as a sequence of preplanned motor commands structured in memory and is believed to serve as a template for planning a class of motions. This generalization is achieved through the use of *parameters* and is guided by *invariant features*. Parameters refer to changeable aspects of a GMP, such as overall duration and overall magnitude of motion. Invariant features are fixed aspects of a GMP, such as order of elements, phasing, and relative magnitude, and define the spatial–temporal structure of motions. Parameters can be altered to produce motion variants that exhibit similar patterns in space and time. Given a specific task, parameters of a GMP are determined by a set of rules (referred to as a schema) to meet the particular needs (Schmidt, 1975).

The goal of our research is to develop human motion simulation models, which utilize GMP-like templates for motion planning. Such templates are obtained by

*Corresponding author. Tel.: +1 513 556 9726; fax: +1 513 556 3390.
E-mail address: woojin.park@uc.edu (W. Park).

0021-9290/$ - see front matter © 2004 Elsevier Ltd. All rights reserved.
doi:10.1016/j.jbiomech.2004.09.035

analyzing real human motion samples. As the first step, this study developed (1) a computer algorithm (symbolic motion structure representation (SMSR) algorithm) that identifies the basic spatial–temporal structure of a human motion, and (2) a method for generalizing a sample motion into a class of motions through parameterization. As an application of the proposed methods, a motion modification (MoM) algorithm is introduced to alter existing reach motions for new target locations.

2. Method

2.1. Symbolic motion structure representation algorithm

The SMSR algorithm analyzes a sample human motion (motion capture data) to identify its basic spatial–temporal structure. A sample motion is assumed to be associated with a linkage system that consists of N rigid body link segments $\mathbf{L} = [l_1 \cdots l_n \cdots l_N]$ and J locally defined joint angles $\boldsymbol{\theta} = [\theta_1 \cdots \theta_j \cdots \theta_J]$. Thus, a sample motion is described as a set of J joint angle–time trajectories $\boldsymbol{\theta}(t) = [\theta_1(t) \cdots \theta_j(t) \cdots \theta_J(t)]$, where t represents time in $[0, T]$. Note that the SMSR algorithm is not specific to a particular linkage system but can be applied to any two- or three-dimensional linkage systems and motions provided that joint angles are locally defined.

The SMSR algorithm resolves each joint angle–time trajectory $\theta_j(t)$ $(j = 1, \ldots, J)$ into a sequence of elemental motion segments in the angle–time domain. Each elemental joint motion corresponds to a monotonically increasing (U), a monotonically decreasing (D), or a stationary (S) motion segment. The algorithm labels each segment with a symbol U, D, or S according to its shape. By concatenating the symbols according to their order in time, the structure of a joint angle trajectory $\theta_j(t)$ is represented by a symbolic string. Successive application of the SMSR algorithm to each of the J joint angle trajectories reveals the structure of a multi-joint motion $\boldsymbol{\theta}(t)$ as a set of J symbolic strings.

The SMSR algorithm consists of the four steps described below. A sample joint angle trajectory obtained from a motion capture experiment (a left elbow flexion/extension angle–time trajectory during a manual handling activity) was used as an example to illustrate each step (Fig. 1a).

2.1.1. Step (1) landmark identification

A joint angle–time trajectory $\theta_j(t)$, where $0 \leqslant t \leqslant T$ is represented as a one-dimensional time-series when obtained from a motion capture experiment. Let us denote such time-series by $\theta_j(k \cdot \Delta t)$, where $k = 0, \ldots, K$. Each point in the time-series, $(k \cdot \Delta t, \theta_j(k \cdot \Delta t))$, is examined as to whether it can be tentatively selected as a segment boundary point (a beginning or end of an elemental motion segment). Such candidates for segment boundary points are called *landmarks*.

The initial and the last point of the time-series are selected as landmarks. All extremes in the time-series are selected as landmarks, as they may be the beginning or end of a monotonically increasing or decreasing segment. A point $(k \cdot \Delta t, \theta_j(k \cdot \Delta t))$ is determined as an extreme when the value of $(\theta_j(k \cdot \Delta t) - \theta_j((k-1) \cdot \Delta t)) \times (\theta_j((k+1) \cdot \Delta t) - \theta_j(k \cdot \Delta t))$ has a negative sign. Also, all points that may be at the beginning or end of a stationary segment are selected as landmarks. A point $(k \cdot \Delta t, \theta_j(k \cdot \Delta t))$ is determined as such landmark, if and only if one of the two slopes, $(\theta_j(k \cdot \Delta t) - \theta_j((k-1) \cdot \Delta t))/\Delta t$ and $(\theta_j((k+1) \cdot \Delta t) - \theta_j(k \cdot \Delta t))/\Delta t$, is zero or close to zero (within a user-specified threshold $\varepsilon_{\text{slope}}$ from zero).

Landmarks were identified for the example joint angle trajectory (Fig. 1b). $\varepsilon_{\text{slope}}$ was set at 1°/min, which is just below the threshold of human proprioception of joint angular motion (Clark et al., 1985, 1986).

2.1.2. Step (2) selection of segment boundary points

Landmarks that reflect noise in a time-series do not qualify as segment boundary points. For example, in Fig. 1b, there are dense clusters of landmarks in plateaus. Demarcating motion segments using all these landmarks would produce too many small segments that merely represent noise. Therefore, segment boundary points are selected from landmarks such that each of the resulting elemental motion segments has a duration longer than a predetermined threshold $\varepsilon_{\text{time}}$.

The first and the last landmarks are selected as segment boundary points. Each landmark between the first and the last is examined consecutively in time as to if:

- it is located farther than $\varepsilon_{\text{time}}$ from at least one of the adjacent landmarks in time, and
- it is located farther than $\varepsilon_{\text{time}}$ from the nearest segment boundary point in time.

A landmark is selected as a segment boundary point if it satisfies the two conditions listed above. The first condition ensures that a segment boundary point adjoins at least one segment. The second ensures that no two consecutive segment boundary points are too close to each other in time.

Segment boundary points were identified for the example joint angle trajectory (Fig. 1c). $\varepsilon_{\text{time}}$ was set at $\frac{1}{6}$s. This forces an elemental motion segment to have a duration longer than or equal to $\frac{1}{6}$s and allows at maximum six motion segments within a 1 s time period. The threshold value of $\frac{1}{6}$s is thought to be sufficiently

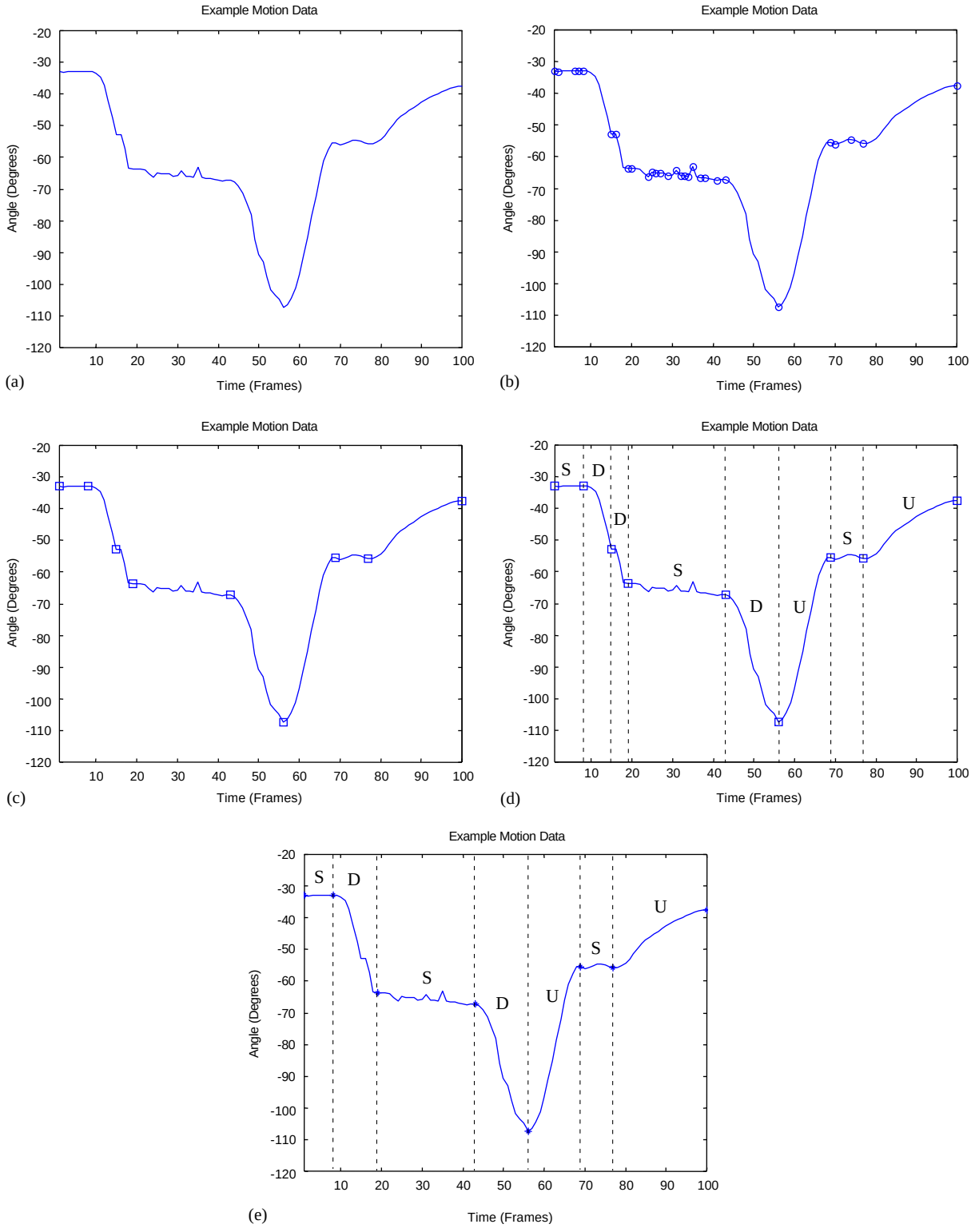

Fig. 1. SMSR algorithm: (a) an example joint angle trajectory, (b) landmark detection, (c) segment boundary point selection, (d) symbol assignment, and (e) redundancy elimination.

small to capture important changes in a normal-paced joint angular motion, as 1 s time period is generally known to allow no more than two movement corrections (Wickens, 1986).

2.1.3. Step (3) symbol assignment

One of the three symbols, 'U', 'D', or 'S', is assigned to each motion segment, according to the associated angular displacement. If the displacement is greater than

or equal to a user-defined threshold $\varepsilon_{\Delta x}$, 'U' is assigned to the segment. If the displacement is less than or equal to $-\varepsilon_{\Delta x}$, 'D' is assigned to the segment. Finally, 'S' will be given, if the displacement is between $-\varepsilon_{\Delta x}$ and $\varepsilon_{\Delta x}$.

Symbol assignment for the example joint angle trajectory is illustrated in Fig. 1d. $\varepsilon_{\Delta x}$ was set at 1° to take into account that angular displacements associated with a 'U' or 'D' segment must be large enough to be perceived by the performer. Indeed, studies on proprioceptive perception have indicated that minimum detectable joint angular displacements vary in the range of 0.3–0.7° across different body joints (Laidlaw and Hamilton, 1937; Grigg et al., 1973).

2.1.4. Step (4) elimination of possible redundancies in a symbolic string

The symbolic string formed in Step (3) may contain redundancies. Indeed, the example joint angle trajectory was described as 'SDDSDUSU', which can be further simplified to 'SDSDUSU' (Fig. 1e). Redundancies are eliminated by merging consecutive segments with identical symbols.

2.2. Motion generalization method

Once a sample motion $\boldsymbol{\theta}(t)$ is analyzed by the SMSR algorithm, it can be generalized to produce an infinite number of similar motion variants. This generalization is based on parametric deformations of the sample motion's joint angle–time trajectories. The segment boundary points identified by the SMSR algorithm are utilized as control parameters for such deformations.

To generate a variant from a sample motion $\boldsymbol{\theta}(t)$, segment boundary points of the sample motion are first moved to new locations in the angle–time space, and then individual segments of the original joint angle trajectories are shifted and proportionally rescaled to fit the new segment boundary points. This deformation method based on 'local proportional scaling' (Kanatani-Fujimoto et al., 1997) can be mathematically described as follows: let (T_i^j, B_i^j) and (τ_i^j, β_i^j) be the original and the new segment boundary point locations in the angle–time space, respectively, where $j = 1, \ldots, J$ and $i = 1, \ldots, I_j$. i is the index of the segment boundary points and I_j denotes the number of segment boundary points in the jth joint angle trajectory $\theta_j(t)$. New joint angle trajectories $\hat{\theta}_j(t)$'s at a given time t $(\tau_i^j \leqslant t \leqslant \tau_{i+1}^j)$ can be represented by

$$\hat{\theta}_j(t) = \beta_i^j + \frac{\beta_{i+1}^j - \beta_i^j}{B_{i+1}^j - B_i^j}\left(\theta_j\left(T_i^j + \frac{T_{i+1}^j - T_i^j}{\tau_{i+1}^j - \tau_i^j}(t - \tau_i^j)\right) - B_i^j\right) \quad \text{when } B_{i+1}^j - B_i^j \neq 0, \text{ and}$$

$$\hat{\theta}_j(t) = \beta_i^j \text{ when } B_{i+1}^j - B_i^j = 0. \tag{1}$$

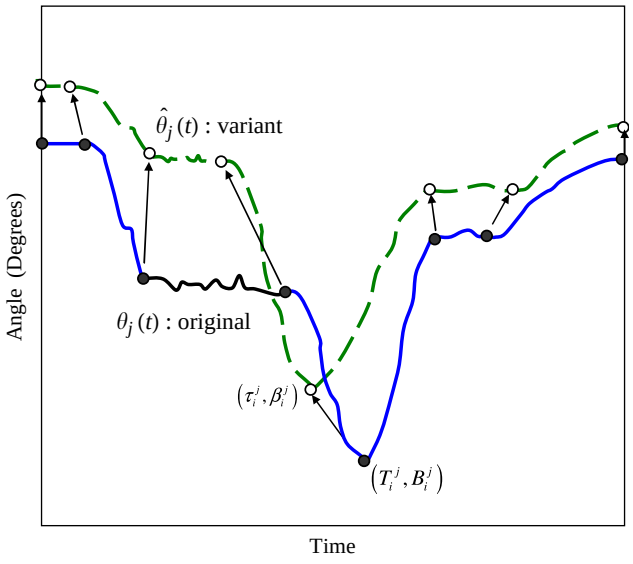

Fig. 2. An example of deriving a variant from a single joint angle trajectory. The solid curve represents an original joint angle trajectory. The filled-in circles represent the segment boundary points of the original joint angle trajectory. The empty circles represent new locations of the segment boundary points. The dashed curve represents a derived variant. The variant maintains the structure ('SDSDUSU') of the original.

An example that illustrates deformation of a single joint angle trajectory based on the above method is provided in Fig. 2. Zhang (2002) used a similar proportional scaling method to alter reach motions and nullify hand position errors.

The new locations of segment boundary points, (τ_i^j, β_i^j)'s, are bound by a motion structure preservation constraint. A new motion $\hat{\boldsymbol{\theta}}(t) = [\hat{\theta}_1(t) \cdots \hat{\theta}_J(t)]$ must maintain the structure of $\boldsymbol{\theta}(t)$ to qualify as a variant of $\boldsymbol{\theta}(t)$. That is, each $\hat{\theta}_j(t)$ must be identical to $\theta_j(t)$ in the symbolic string representation. This constraint forces a class of motions derived from a sample motion to retain the sample motion's basic structure in the joint angle–time trajectories.

3. Motion modification algorithm

3.1. Motion modification (MoM) algorithm

The MoM algorithm (Park et al., 2004) adapts an existing target reach motion for newly given target locations. The algorithm can be used as a general motion simulation method provided that a motion library or a motion database exists. Three types of input data are assumed to be given for an MoM problem: (1) anthropometric body segment dimensions, $\mathbf{L} = [l_1 \cdots l_n \cdots l_N]$; (2) a sample motion, $\boldsymbol{\theta}(t) = [\theta_1(t) \cdots \theta_j(t) \cdots \theta_J(t)]$, where $0 \leqslant t \leqslant T$; (3) a new target

location, **E**. The goal is to modify $\boldsymbol{\theta}(t)$ to derive a new motion that attains the new target position **E**.

The sample motion $\boldsymbol{\theta}(t)$ is first analyzed by the SMSR algorithm to identify the structure and the segment boundary points, (T_i^j, B_i^j)'s ($j = 1, \ldots, J$ and $i = 1, \ldots, I_j$). The output motion to be generated is a modification of $\boldsymbol{\theta}(t)$, $\hat{\boldsymbol{\theta}}(t) = [\hat{\theta}_1(t) \cdots \hat{\theta}_j(t) \cdots \hat{\theta}_J(t)]$, where $0 \leqslant t \leqslant T$. As described in Section 2.2, $\hat{\boldsymbol{\theta}}(t)$ is obtained by relocating (T_i^j, B_i^j)'s to new locations (τ_i^j, β_i^j)'s and deforming $\boldsymbol{\theta}(t)$ accordingly, based on Eq. (1). Therefore, solving an MoM problem amounts to determining (τ_i^j, β_i^j)s ($j = 1, \ldots, J$ and $i = 1, \ldots, I_j$).

The output motion $\hat{\boldsymbol{\theta}}(t)$ must satisfy the following constraints:

- *Target acquisition constraint*: $\hat{\boldsymbol{\theta}}(t)$ must locate the hand at the intended position **E**. That is,

$$\mathbf{F}(\hat{\boldsymbol{\theta}}(T), \mathbf{L}) = \mathbf{E}, \tag{2}$$

  where **F** represents the forward kinematics equation for calculating hand position.
- *Joint range of motion constraint*: Each joint angle trajectory of $\hat{\boldsymbol{\theta}}(t)$ must reside within the joint angle's normal range of motion. This is expressed by

$$L_j \leqslant \hat{\theta}_j(t) \leqslant U_j \text{ for } j = 1, \ldots, J \text{ and } 0 \leqslant t \leqslant T, \tag{3}$$

  where L_j and U_j represent the lower and the upper limit of the jth joint angle value, respectively. Normal joint range of motion data are extracted from Webb Associates (1978).
- *Body balance maintenance constraint*: A static balance condition is employed as a constraint to ensure body balance maintenance of the output motion. To maintain balance, the vertical projection of the whole-body center of mass must reside within the base of support (BoS) formed by the feet. This static balance condition is expressed by

$$\mathbf{P}_{\mathbf{com}}(\hat{\boldsymbol{\theta}}(t), \mathbf{L}) \in \text{BoS} \text{ for } 0 \leqslant t \leqslant T, \tag{4}$$

  where $\mathbf{P}_{\mathbf{com}}$ and BoS represent the vertical projection of the whole-body center of mass on the floor and the BoS defined by the feet, respectively. Dempster (1955) provides body segment mass distribution and center location data necessary for computing $\mathbf{P}_{\mathbf{com}}(t)$ as a function of a posture $\hat{\boldsymbol{\theta}}(t)$ at time t.
- *Motion structure preservation constraint*: The symbolic string representation of $\hat{\boldsymbol{\theta}}(t)$ must be identical to that of $\boldsymbol{\theta}(t)$:

$$\text{STRING } (\hat{\theta}_j(t)) = \text{STRING } (\theta_j(t)) \text{ for all } j. \tag{5}$$

The above constraints (Eqs. (2)–(5)) in general do not completely determine (τ_i^j, β_i^j)'s. In other words, there exists an infinite number of possible ways for locating (τ_i^j, β_i^j)'s that satisfy the above constraints. To resolve this indeterminacy, an optimization-based approach was devised (Park et al., 2004). First, the final posture of the new motion $\hat{\boldsymbol{\theta}}(T)$, which is the set of the very last boundary points $[\beta_{I_1}^1 \cdots \beta_{I_j}^j \cdots \beta_{I_J}^J]$, is determined by solving the following minimization problem:

$$\begin{aligned} &\text{Minimize} && \sum_{j=1}^{J} (\hat{\theta}_j(T) - \theta_j(T))^2 \\ &\text{s.t.} && \text{the four constraints shown in Eqs. (2)}-\text{(5).} \end{aligned} \tag{6}$$

The new final posture $\hat{\boldsymbol{\theta}}(T)$ determined by the above method resembles the original motion's final posture $\boldsymbol{\theta}(T)$ the most. Once the new final posture $\hat{\boldsymbol{\theta}}(T)$ is determined, the new joint angle trajectories that link the initial posture $\boldsymbol{\theta}(0)$ to the new final posture $\hat{\boldsymbol{\theta}}(T)$ are determined by solving the following minimization problem for (τ_j^i, β_j^i)'s for each j ($i = 1, \ldots, (I_j - 1)$):

$$\begin{aligned} &\text{Minimize} && \int_0^T (\dot{\hat{\theta}}_j(t) - \dot{\theta}_j(t))^2 \, \mathrm{d}t \\ &\text{s.t.} && \hat{\theta}_j(0) = \theta_j(0), \\ & && \hat{\theta}_j(T) \text{ is given as a constant} \\ & && \quad \text{by solving Eq. (6),} \end{aligned} \tag{7}$$

where $\dot{\hat{\theta}}_j(t)$ and $\dot{\theta}_j(t)$ denote the first time derivatives of $\hat{\theta}_j(t)$ and $\theta_j(t)$.

The new motion $\hat{\boldsymbol{\theta}}(t)$ determined by the above method resembles the original motion $\boldsymbol{\theta}(t)$ the most in the joint angular velocity domain. Nonlinear optimization methods used for solving the minimization problems shown above have been previously described (Park et al., 2004).

3.2. Motion modification examples

Two sample reach motions (right-handed standing reaches) were modified by the MoM algorithm for new target locations. The sample motions were extracted from an existing motion database (Chaffin, 2001). The first motion (Fig. 3a) was a side reach performed by a male subject (177 cm, 81 kg). The second motion (Fig. 3b) was a forward, downward reach performed by another male subject (191 cm, 76 kg).

The motions were recorded at a sampling frequency of 25 Hz, using a custom motion capture system, utilizing both the optical MacReflex™ and the electromagnetic Flock-of-Birds™ system (Fig. 4a). Internal joint center locations were derived from marker position and orientation data to construct a kinematic linkage system (Fig. 4b). The linkage system consisted of 17 constant-length body segment links and 39 local Euler angles. While performing the reaches, the subjects were asked to maintain the left ball-of-foot at a fixed position on the floor, which served as the origin of the linkage system.

Each motion was modified for six new target locations, which were 30 cm away from the original in different directions: upward, downward, forward, backward, and sideways. This set of new target locations

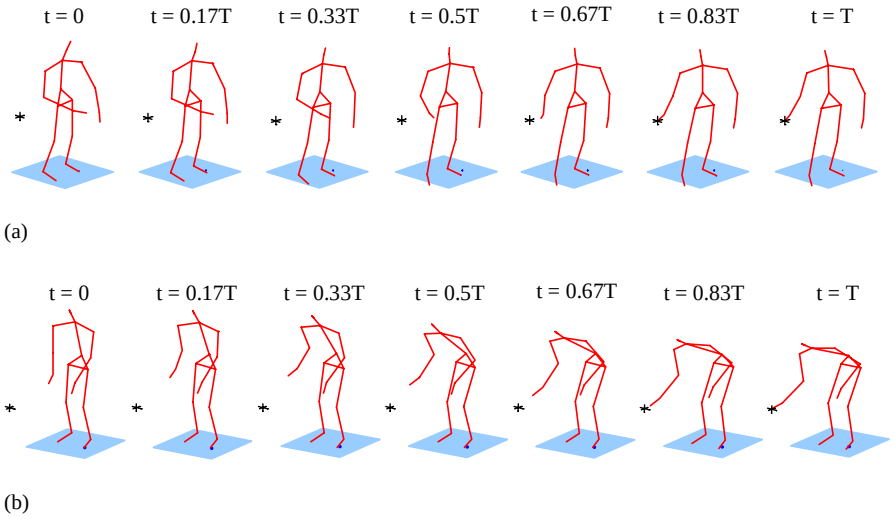

Fig. 3. Two sample reach motions: (a) a side reach and (b) a forward, downward reach. The crosshairs represent the reach targets.

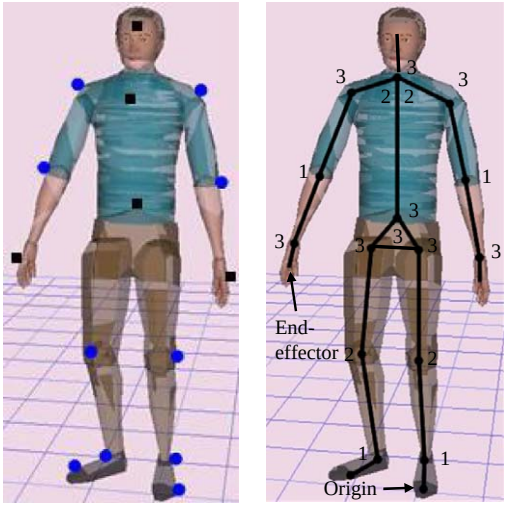

Fig. 4. Surface marker locations and resulting kinematic linkage: (a) the circles and squares represent 10 optical and five electromagnetic markers, respectively, and (b) derived internal joint centers, link segments, and joint degrees of freedom.

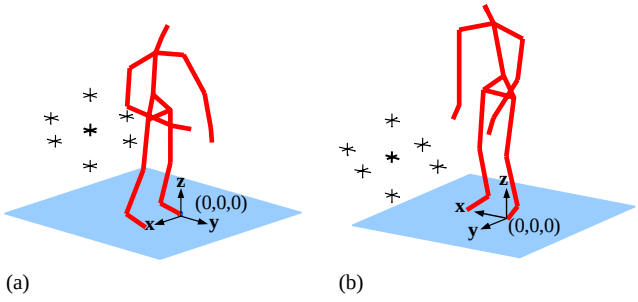

Fig. 5. Six new target locations for MoM: (a) a side reach (b) a forward, downward reach. The initial standing postures at $t = 0$ are depicted. The thick crosshair in the middle represents the original target location. The thin crosshairs represent new target locations 30 cm away from the original.

tested the robustness of the MoM algorithm in producing realistic motion variants for novel scenarios (Fig. 5).

MoM results are presented in Figs. 6 and 7 for the side and forward–downward motions, respectively. The original reaches (a) are followed by the six modifications (b–g).

4. Discussion

Inspired by the GMP theory, the current study presented a SMSR algorithm for identifying basic spatial–temporal structure of human motion and a method for motion generalization. An MoM algorithm that alters reach motions for new target locations was developed based on the SMSR algorithm and the motion generalization method. Two MoM examples (Figs. 6 and 7) demonstrated that the MoM algorithm can generate realistic motion variants for various new scenarios.

The proposed SMSR algorithm and the motion generalization method provide a basis for developing various GMP-based motion simulation models and exploring ideas and hypotheses related to the GMP theory through simulation. Of particular interest is the question of how a schema (Schmidt, 1975) can be modeled. The MoM algorithm employed a schema that determines parameters for novel task requirements by minimizing deviations from existing sample motions in the final posture and the joint angular velocity profiles (Eqs. (6) and (7)). This human performance imitation approach was found to produce realistic motion

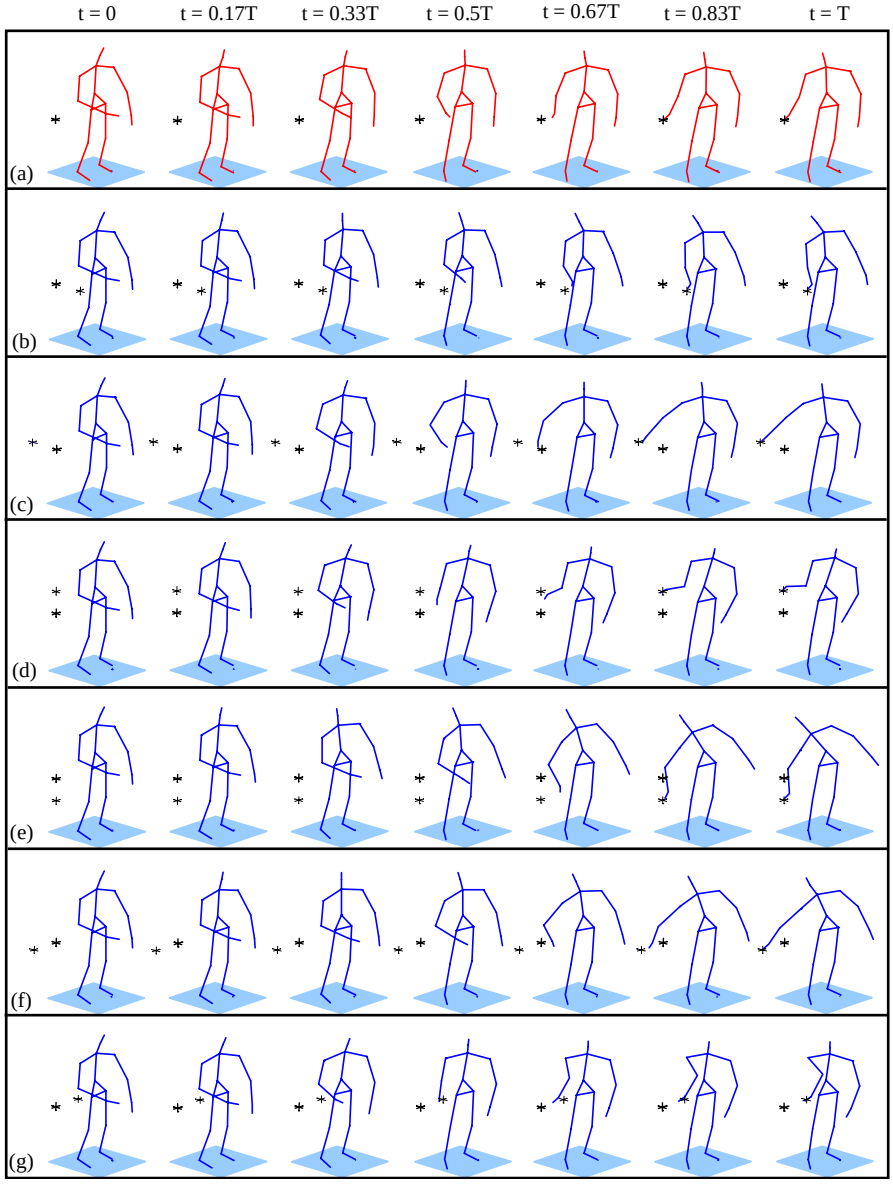

Fig. 6. A side reach (a) and its variants generated for new target locations (b–g). The thick crosshairs represent the original target location. The thin crosshairs represent the new target locations.

variants, as shown in Figs. 6 and 7. Nonetheless, various kinematic and biomechanical criteria, including minimum jerk (Flash and Hogan, 1985), minimum torque change (Uno et al., 1989), and minimum energy (Alexander, 1997), may be able to simulate human reach motions in a robust manner when utilized as possible schemata. These methods assume a control of an "output" variable while our method assumes implicitly a control of movement parameters, which is compatible with the frequent absence of minimization in voluntary human movements. A simple example of no-minimization is illustrated by radical alternatives such as stoop and squat lifting that can be used to perform the same task. Nevertheless, comparison of alternative schemata in terms of robustness and extrapolation capabilities may provide further insights into the principles of human motion planning.

The methods proposed in the present study could be related to the Kendama (a cup-and-ball game) learning algorithm developed by Miyamoto et al. (1996), which utilizes existing human motion data to teach an anthropomorphic robot arm to play the game. Given a sample human motion, the algorithm first extracts a set of via-points by analyzing the hand position and orientation time trajectories. Then, the motion data are adjusted to fit the robot arm geometry. Finally, spatial and temporal positions of the via-points are adjusted by supervised learning until the recalculated robot arm motion fulfills the task goal. Via-points are

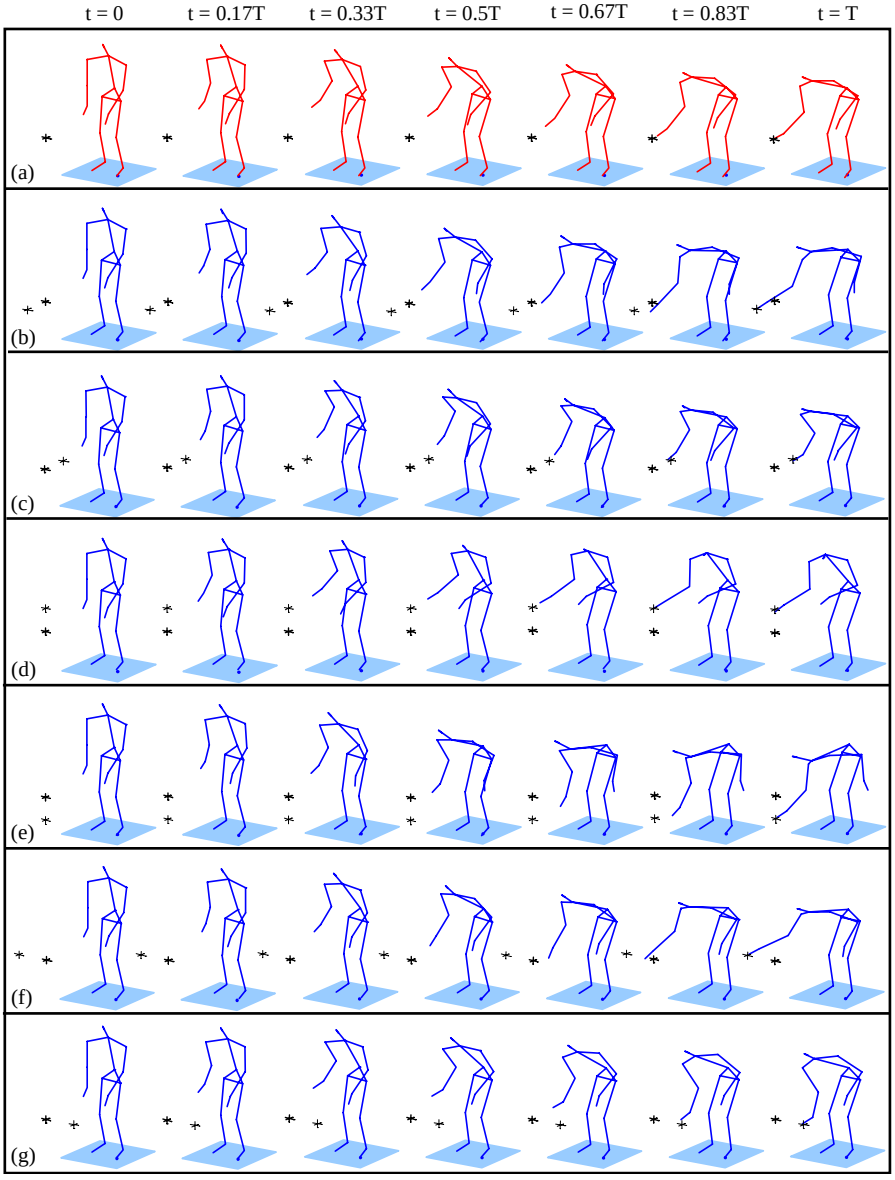

Fig. 7. A forward, downward reach (a) and its variants generated for new target locations (b–g). The thick crosshairs represent the original target location. The thin crosshairs represent the new target locations.

similar to segment boundary points in that they characterize fundamental motion structure and are utilized as control parameters for modifying motions. However, the methods proposed in this study and the Kendama algorithm differ in the domain of motion structure representation. The former represents motion structure in the angle–time space while the latter is based on hand motion over time. Comparison of the two methods in the performance of human motion prediction and robot learning may provide further insights into the advantages and disadvantages of each motion representation scheme. Despite the difference, the two approaches collectively support the notion of GMP-based motion simulation and parametric motion planning.

The SMSR algorithm uses three user-defined parameters: $\varepsilon_{\text{slope}}$, $\varepsilon_{\text{time}}$, and $\varepsilon_{\Delta x}$. Although the current study provided suggested values for the three parameters ($\varepsilon_{\text{slope}} = 1^\circ/\text{min}$, $\varepsilon_{\text{time}} = \frac{1}{6}\text{s}$, and $\varepsilon_{\Delta x} = 1^\circ$), they are applicable mainly for normal-paced motions in daily or work activities. Depending on the motion type (e.g., high-speed sports or dance movements), the parameter values can be adjusted.

References

Alexander, R.M., 1997. A minimum energy cost hypothesis for human arm trajectory. Biological Cybernetics 76, 97–105.

Chaffin, D.B., 2001. On simulating human reach motions for ergonomic analyses. In: Proceedings of the International

Conference on Computer-Aided Ergonomics and Safety. International Ergonomics Association, Maui.

Clark, F.J., Burgess, R.C., Chapin, J.W., Lipscomb, W.T., 1985. Role of intramuscular receptors in the awareness of limb position. Journal of Neurophysiology 54 (6), 1529–1540.

Clark, F.J., Burgess, R.C., Chapin, J.W., 1986. Proprioception with the proximal interphalangeal joint of the index finger. Evidence for a movement sense without a static-position sense. Brain 109 (6), 1195–1208.

Dempster, W.T., 1955. Space Requirements of the Seated Operator, WADC-TR-55-159. Aerospace Medical Research Laboratories, Ohio.

Flash, T., Hogan, N., 1985. The coordination of arm movements: an experimentally confirmed mathematical model. Journal of Neuroscience 5, 1688–1703.

Grigg, P., Finerman, G.A., Riley, L.H., 1973. Joint-position sense after total hip replacement. Journal of Bone and Joint Surgery 55A, 1016–1025.

Kanatani-Fujimoto, K., Lazareva, B.V., Zatsiorsky, V.M., 1997. Local proportional scaling of time-series data: method and applications. Motor Control 1 (1), 20–43.

Laidlaw, R.W., Hamilton, M.A., 1937. A study of thresholds in appreciation of passive movement among normal control subjects. Bulletin of the Neurological Institute of New York 6, 268–273.

Miyamoto, H., Schaal, S., Gandolfo, F., Gomi, H., Koike, Y., Osu, R., Nakano, E., Wada, Y., Kawato, M., 1996. A Kendama learning robot based on bi-directional theory. Neural Networks 9 (8), 1281–1302.

Park, W., Chaffin, D.B., Martin, B.J., 2004. Toward memory-based human motion simulation: development and validation of a motion modification algorithm. IEEE Transactions on Systems, Man, and Cybernetics, Part A: Systems and Humans 34 (3), 376–386.

Schmidt, R.A., 1975. A schema theory of discrete motor skill learning. Psychological Review 82, 225–260.

Schmidt, R.A., Lee, T.D., 1999. Motor control and learning: a behavioral emphasis. Human Kinetics.

Uno, Y., Kawato, M., Suzuki, R., 1989. Formation and control of optimal trajectory in human multijoint arm movement—minimum torque-change model. Biological Cybernetics 61, 89–101.

Webb Associates, 1978. Anthropometric Source Book, vol. I, NASA Ref. 1024, Nat'l Aero. Space Admin. (Chapters VI and VII).

Wickens, C.D., 1986. The effects of control dynamics on performance. In: Boff, K.R., Kauffman, L., Thomas, J.P. (Eds.), Handbook of Perception and Human Performance. Wiley, New York pp. 39-1–39-60.

Zhang, X., 2002. Deformation of angle profiles in forward kinematics for nullifying end-point offset while preserving movement properties. ASME Journal of Biomechanical Engineering 124, 490–495.